Supplementary Information (SI) for Journal of Materials Chemistry A.
This journal is © The Royal Society of Chemistry 2025

Supporting Information

Reversible two-electron redox conversion enabled by an activated electrode and stabilized inter-halogen electrolyte for high performance zinc-iodine flow battery

Jing Yang[a,b], Hui Yan[a,b], Ying Li [a], Ao Tang[a,*]

[a] Institute of Metal Research, Chinese Academy of Sciences, Shenyang, China

[b] School of Materials Science and Engineering, University of Science and Technology of China, Shenyang, China

*Corresponding author: Ao Tang

Email: a.tang@imr.ac.cn Tel: +86-024-81083919 Fax: +86-024-23998320

Supplementary Figures

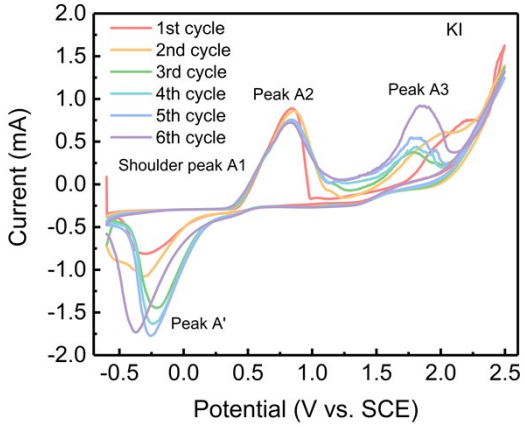

Figure S1 Cyclic voltammograms of redox reactions in pristine KI electrolyte at a scan rate of 20 mV s^{-1}.

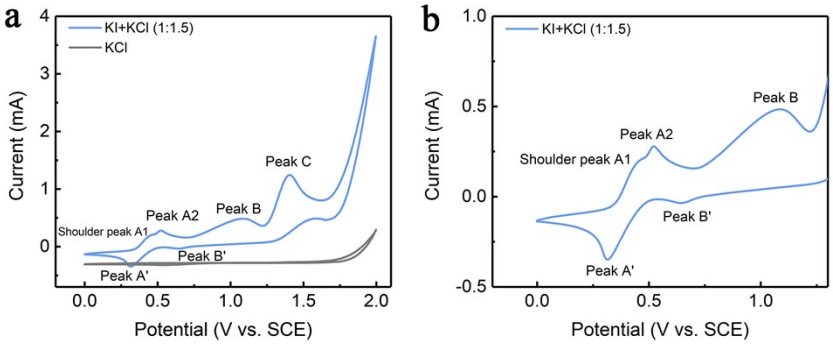

Figure S2 (a) Cyclic voltammograms of redox reactions in pristine KI+KCl (1:1.5) and KCl electrolytes at a scan rate of 20 mV s^{-1}; (b) Magnification of (a).

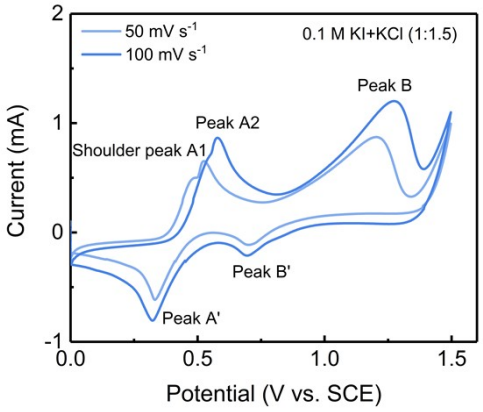

Figure S3 Cyclic voltammograms of redox reactions in 0.1 M KI+KCl (1:1.5) electrolyte at different scan rates.

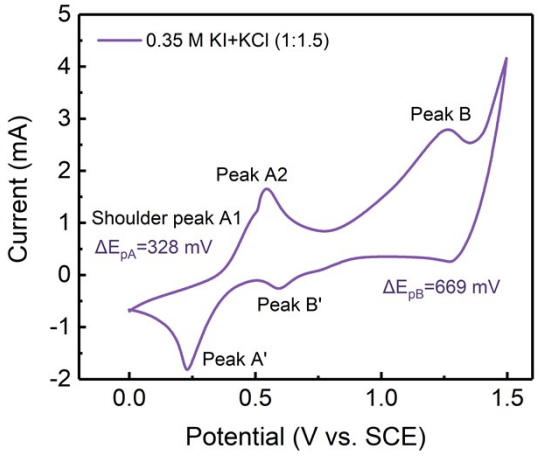

Figure S4 Cyclic voltammograms of redox reactions in 0.35 M KI+KCl (1:1.5) electrolyte at a scan rate of 100 mV s^{-1}.

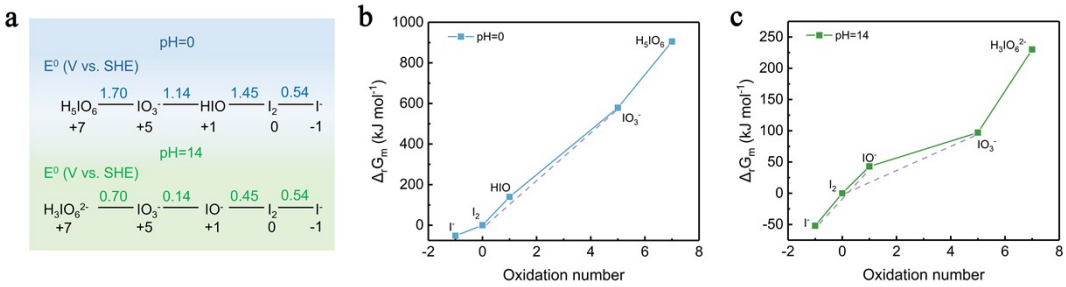

Figure S5 (a) Element potential diagram of iodine; Free energy-oxidation number diagram of iodine system at (b) acid solutions and (c) alkaline solutions.

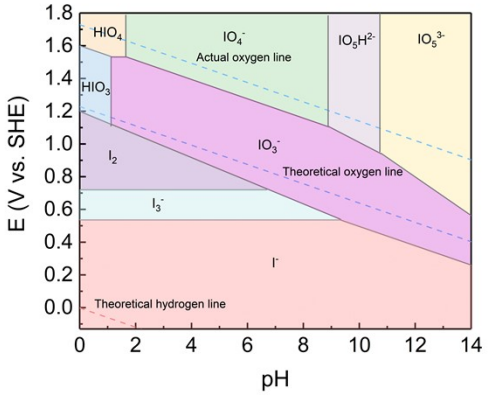

Figure S6 E-pH diagram of I-H_2O system.

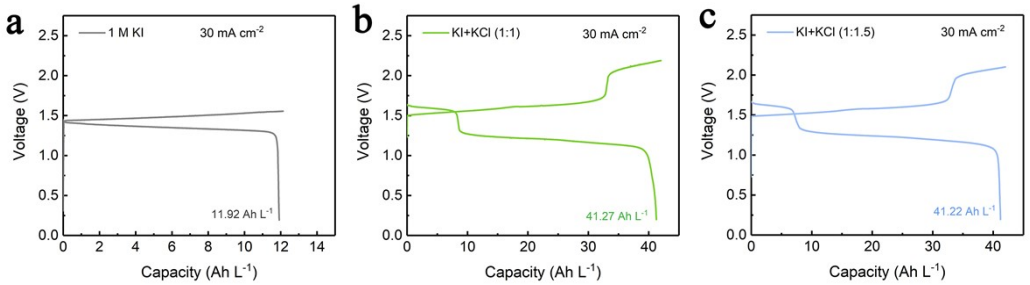

Figure S7 Galvanostatic voltage profiles of the ZIFB with (a) KI, (b) KI+KCl (1:1) and (c) KI+KCl (1:1.5) electrolytes as posolyte at a current density of 30 mA cm^{-2}.

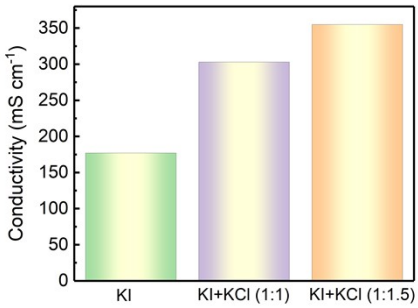

Figure S8 Conductivity of three aqueous electrolytes with different concentrations of Cl^- additives.

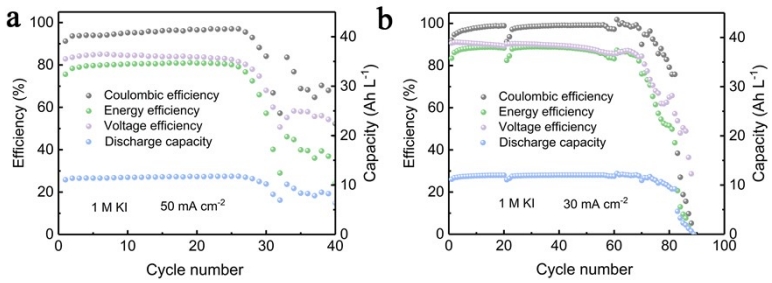

Figure S9 The discharge capacity and efficiencies of ZIFB using KI electrolytes at a current density of (a) 50 mA cm^{-2} and (b) 30 mA cm^{-2}.

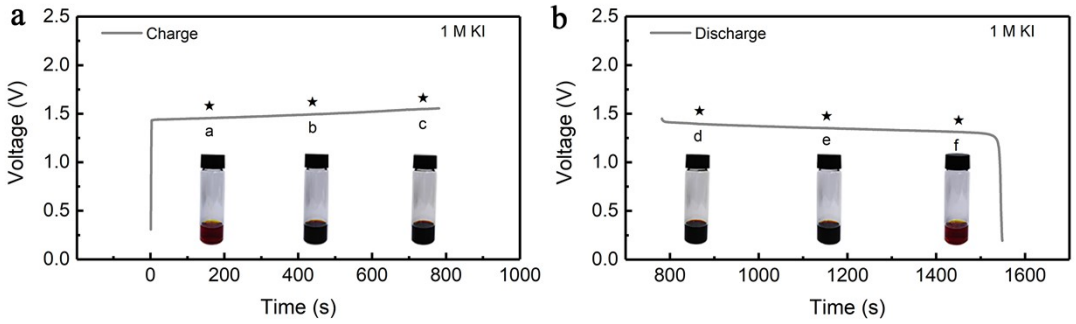

Figure S10 (a) charge and (b) discharge curves and their corresponding photographs of the KI electrolyte at different stages.

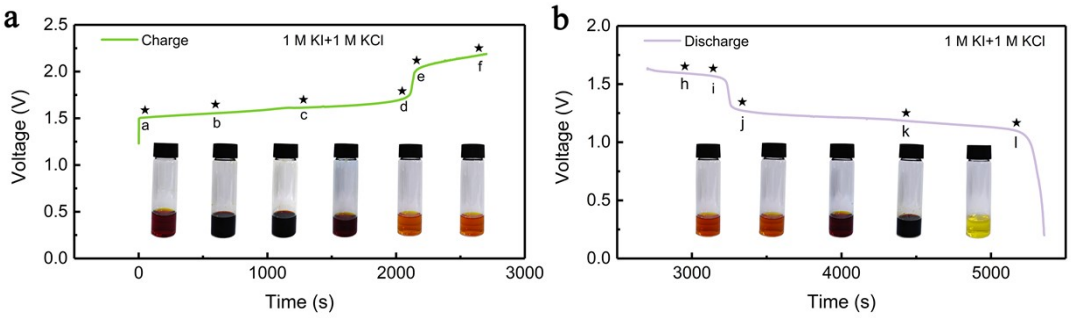

Figure S11 (a) charge and (b) discharge curves and their corresponding photographs of the KI+KCl (1:1) electrolyte at different stages.

Figure S12 Photography of the KI+KCl electrolyte at stage d.

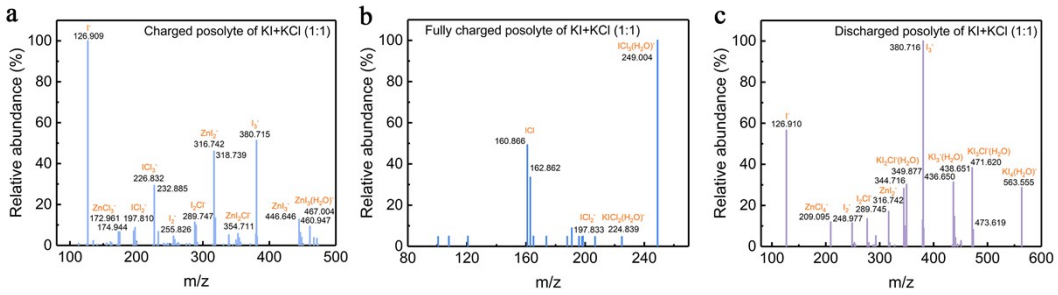

Figure S13 ESI-MS of the (a) charged posolyte, (b) fully charged posolyte and (c) discharged posolyte.

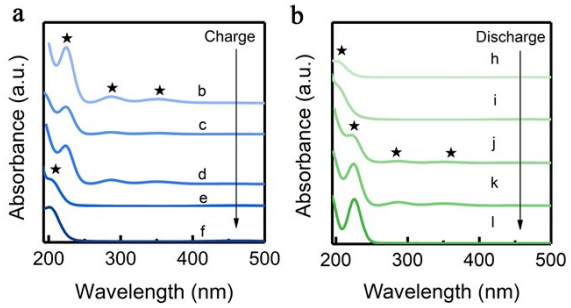

Figure S14 UV-vis spectra of the KI+KCl (1:1) electrolytes at different (a) charge and (b) discharge states.

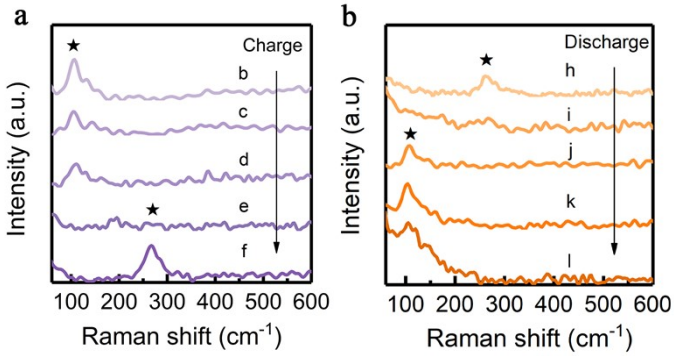

Figure S15 Raman spectrum of KI+KCl (1:1) electrolytes with different stages of (a) charge and (b) discharge states.

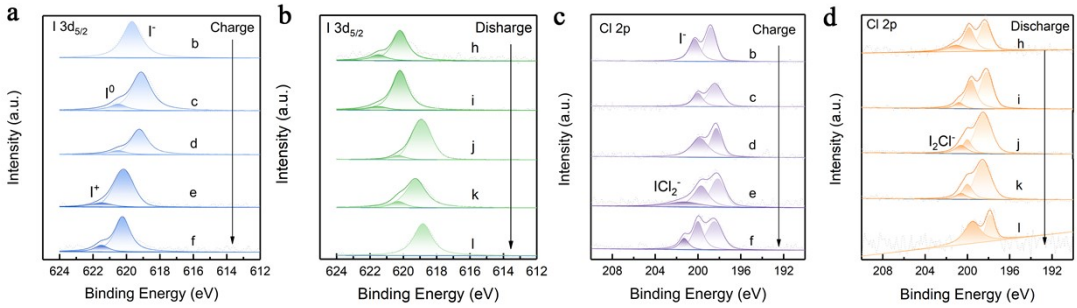

Figure S16 The high-resolution XPS (a-b) I $3d_{5/2}$ and (c-d) Cl 2p spectra of KI+KCl (1:1) electrolytes at charge and discharge states.

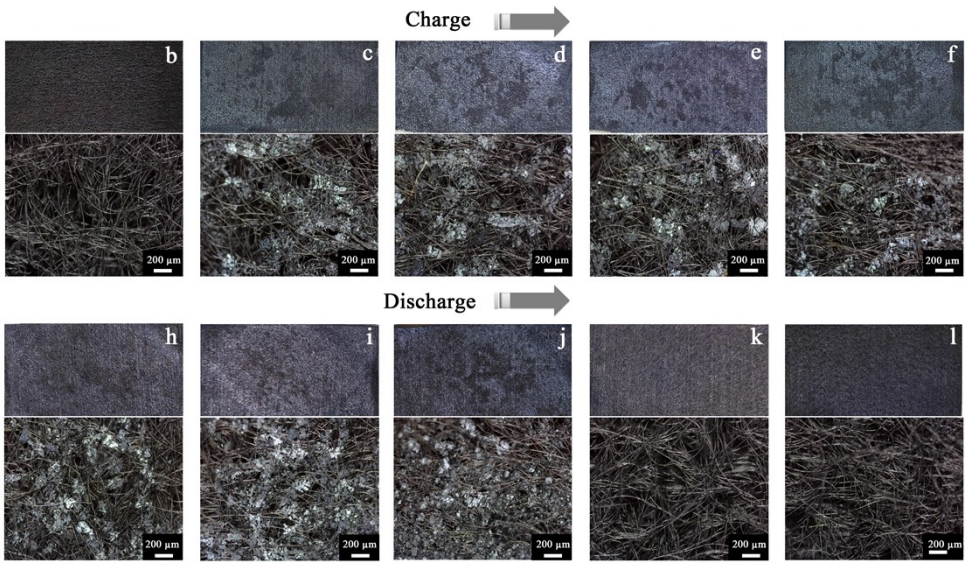

Figure S17 The morphologies of iodine species on carbon felt in KI+KCl (1:1) electrolyte at charge and discharge stages in a battery system.

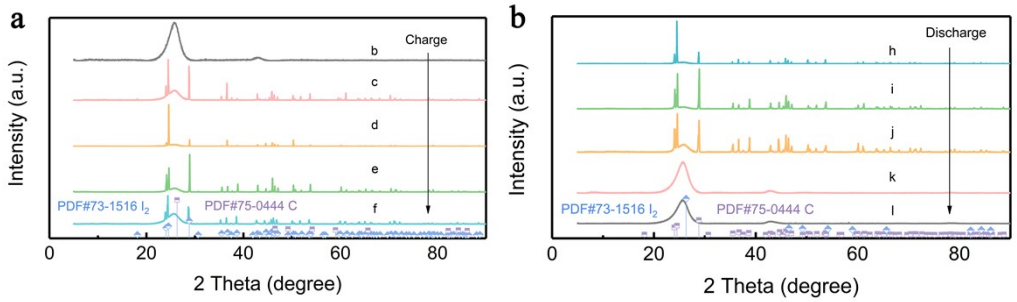

Figure S18 XRD spectra of the products from (a) charge and (b) discharge steps in KI+KCl (1:1) electrolytes.

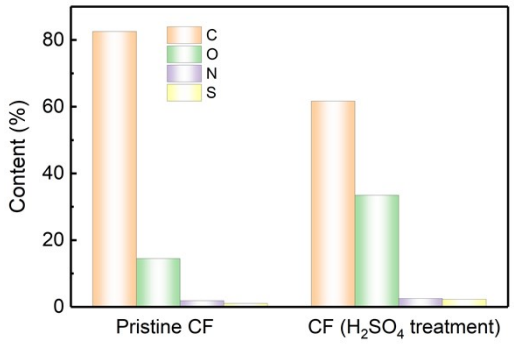

Figure S19 Composition and content of elemental on the pristine carbon felt and carbon felt treated in sulfuric acid.

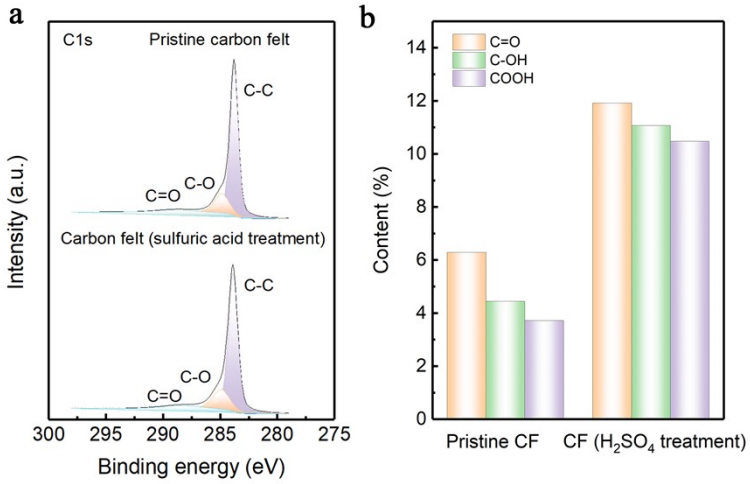

Figure S20 (a) The high-resolution C 1s XPS spectra of the pristine carbon felt and carbon felt treated in sulfuric acid. (b) Elemental composition and content of oxygen functional groups on the samples.

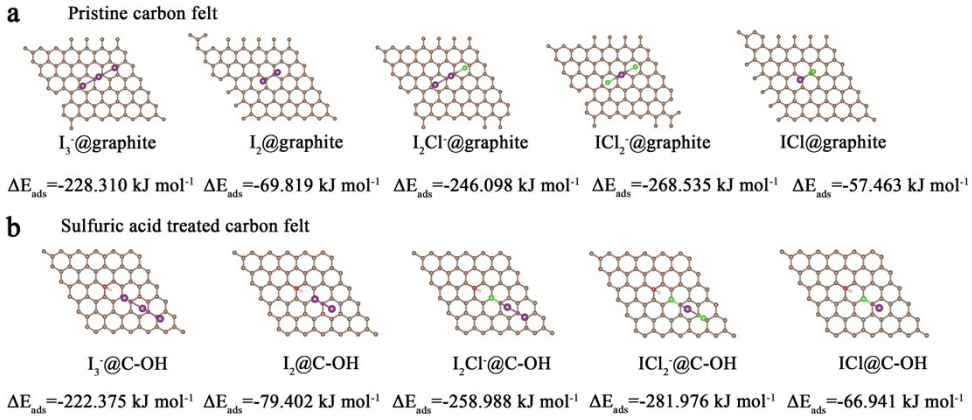

Figure S21 Adsorption energy and charge difference analysis (top view) at (a) pristine carbon felt and (b) sulfuric acid treated carbon felt.

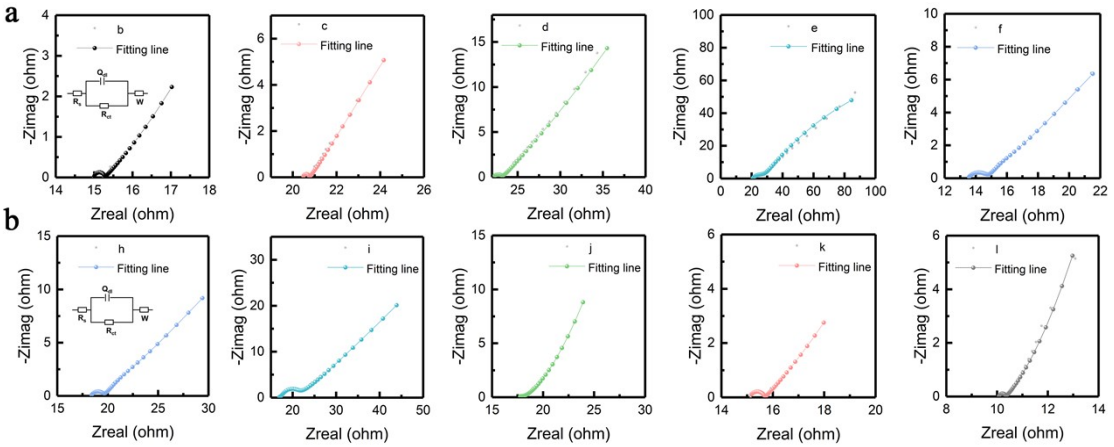

Figure S22 EIS results of the ZIFB at (a) charge and (b) discharge stages in KI+KCl (1:1) electrolytes.

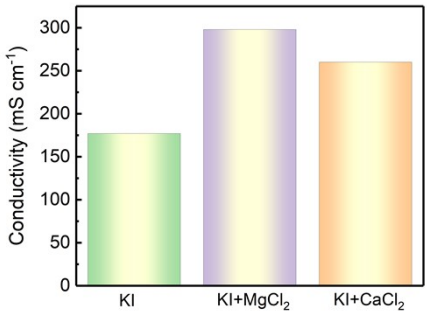

Figure S23 Conductivity of various electrolytes.

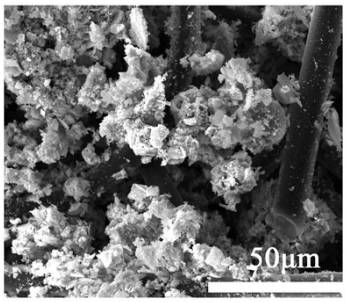

Figure S24 Cross-sectional SEM images of the carbon felt after long cycling.

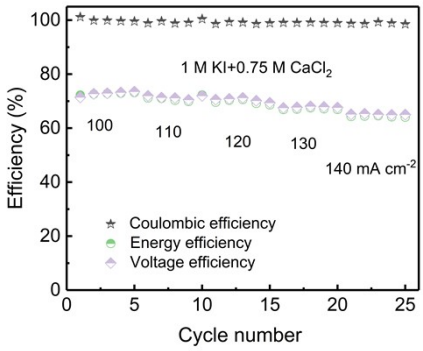

Figure S25 Rate performance of the ZIFB adopting1 M KI+0.75 M $CaCl_2$ electrolytes cycled at various current densities from 100 mA cm^{-2} to 140 mA cm^{-2}.

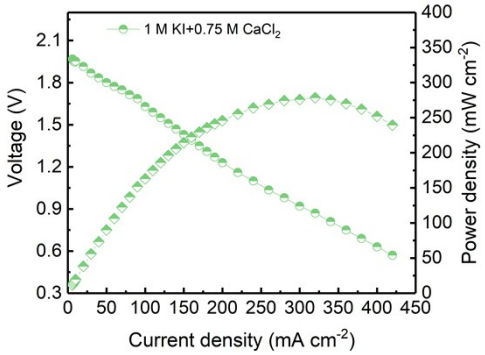

Figure S26 Discharge polarization and calculated power density curves of the ZIFB with 1 M KI+0.75 M $CaCl_2$ electrolytes at a state of charge (SOC) of 90%.

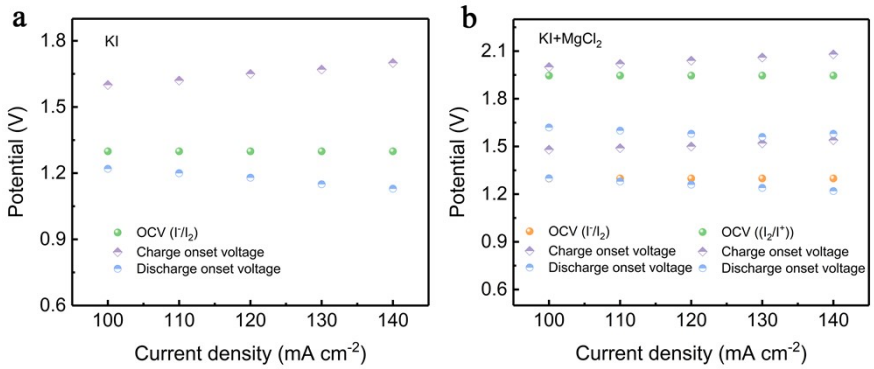

Figure S27 The charge and discharge onset voltage of (a) KI and (b) KI+$MgCl_2$ electrolytes at different current density.

Supplementary Tables

Table S1 Calculated binding energy of different molecules

Molecules	Energy (Hatree)	E_B (Hatree)	E_B (kcal mol^{-1})
Cl^-	−460.404970686	/	/
H_2O	−76.4709073298	/	/
I^-	−297.993488592	/	/
I_2	−595.631366172	/	/
I_2Cl^-	−1056.06303036	/	/
I_3^-	−893.651463733	/	/
ICl	−758.033231894	/	/
ICl_2^-	−1218.47634406	/	/
I-Cl	−758.033231894	/	/
I_2-Cl^-	−1056.06303036	−0.02669350200	−16.75017250507
I_2-I^-	−893.651463733	−0.026608969000	−16.697367528221
I_2-H_2O	−672.104600954	−0.002327452200	−1.46047625554
ICl-Cl^-	−1218.47634406	−0.0381414799	−23.93377869995
ICl-H_2O	−834.5060364	−0.001897153	−1.190463633
ICl_2^--H_2O	−1294.95391906	−0.006667670200	−4.183963050572

Note:

The binding energy (EB) between iodine species and water molecular/halogen ions is defined as following:

$$E_B = E_{Complex} - E_c - E_m$$

where $E_{Complex}$ is the total energy of complex, E_c is the total energy of iodine species, E_m is the total energy of various halogen ions.

Table S2 Calculated adsorption energy of different molecules

Molecules	Energy (Hatree))	E_{absorb} (kJ mol^{-1})
I_3^-	−1136.68457	/
I_2	−757.794257	/
I_2Cl^-	−837.126605	/
ICl_2^-	−537.567979	/
ICl	−458.232143	/
C (001)	−1328.10449	/
I_3^-@C (001)	−2464.87602	−228.310
I_2@C (001)	−2085.92534	−69.819
I_2Cl^-@C (001)	−2165.32483	−246.098
ICl_2^-@C (001)	−1865.77475	−268.535
ICl @C (001)	−1786.35852	−57.463
C (OH)	−1370.81921	/
I_3^-@C (OH)	−2507.58848	−222.375
I_2@C (OH)	−2128.64371	−79.402
I_2Cl^-@C (OH)	−2208.04446	−258.988
ICl_2^-@C (OH)	−1908.49459	−281.976
ICl@C (OH)	−1829.07685	−66.941

Note:

The absorbed energy between C slab and different molecules was defined by following equation:

$$E_{absorb.} = E_{C\text{-}slab+molecules} - E_{C\text{-}slab} - E_{molecules}$$

Table S3 Cycling performance of ZIFB adopting 1M I^- electrolytes at various current density

Electrolytes	Current density ($mA\ cm^{-2}$)	Charge voltage (V)	Discharge voltage (V)
KI	100	1.72	1.05
	120	1.78	0.99
	140	1.83	0.93
KI+$MgCl_2$	100	1.62/2.02	1.22/1.55
	120	1.65/2.06	1.20/1.51
	140	1.70/2.10	1.17/1.44

Table S4 Discharge capacity and energy density of ZIFB adopting 1M I^- electrolytes at various current density

Electrolytes	Current density ($mA\ cm^{-2}$)	Discharge capacity ($Ah\ L^{-1}$)	Energy density ($Wh\ L^{-1}$)
KI	100	11.89	11.66
	120	11.36	10.82
	140	9.03	8.10
KI+$MgCl_2$	100	39.10	48.29
	120	35.90	43.65
	140	36.23	43.00

Table S5 Cycling performance of ZIFB adopting various concentration I^- electrolytes at current density of 100 mA cm^{-2}

Electrolytes	Concentration (M)	Discharge capacity (Ah L^{-1})	Energy density (Wh L^{-1})
KI	1	11.89	11.66
	2	27.07	27.82
	6	61.06	61.28
KI+$MgCl_2$	1	39.10	48.29
	2	73.22	93.82
	2.6	110.56	132.25